CO2 solubility in formation water under sequestration conditions

CO_2 Solubility in formation water under sequestration conditions

Pezhman Ahmadi[a], Antonin Chapoy[a,b,]*

[a] *Hydrates, Flow Assurance & Phase Equilibria Research Group, Institute of Petroleum Engineering, Heriot-Watt University, Edinburgh EH14 4AS, Scotland, UK*

[b] *Mines ParisTech, CTP – Centre Thermodynamique des procédés, 35 rue St Honoré 77305 Fontainebleau, France*

Abstract

A high pressure experimental setup was used to measure the solubility of CO_2 in an aqueous solution of different salts (salinity: ~ 80000 ppm) at temperatures from (300 to 424) K and pressures up to 41 MPa. To ensure the validity of the experimental results and procedures, CO_2 solubilities in deionised water were measured at the same pressure and temperature conditions. For both cases, experimental results were compared against predictions of the simplified cubic plus association equation of state (sCPA-EoS) [1] and Duan model [2]. Furthermore, the measured solubilities in deionised water were compared with literature experimental data.

The average absolute deviation (%AAD) of all the measured solubilities in the mixed salts aqueous solution in comparison with predictions of the sCPA-EoS and Duan model were found to be 6.88% and 4.04%, respectively. A similar comparison was also performed for the measured CO_2 solubilities in deionised water. The average absolute deviation between experimental results and predictions of the sCPA-EoS and Duan model were calculated to be 7.74% and 4.19%, respectively. The percentage average expanded uncertainty (with 95% level of confidence, k=2) for measurements conducted in deionised water and mixed salt aqueous solution were found to be 1.20% and 1.57%, respectively.

Keywords: CO_2 solubility; Water; NaCl; Experimental measurement; Thermodynamic Modelling

* Corresponding author, Email: a.chapoy@hw.ac.uk

1. Introduction

Accurate knowledge of CO_2 solubility in aqueous solutions has always been of great interest for various applications in different industries. For instance, among the methods used in Carbon Capture and Sequestration (CCS), injection of CO_2 into deep aquifers, is one of the most practical methods for reducing CO_2 emission. Phase behaviour of the CO_2 in contact with an aqueous phase and CO_2 solubility in the aqueous phase, are of the most relevant information required in this method. Moreover, effects of reservoir condition (e.g. reservoir temperature and pressure) and aqueous phase salinity on CO_2 dissolution are some of the key parameters that need to be estimated accurately for planning any CO_2 storage project. Apart from geological storage, accurate estimation of CO_2 solubility in fluids is essential for design, control and optimisation of many industrial processes such as gas sweetening and decontamination of wastewaters containing dissolved acid gases.

Although different thermodynamic models have been developed to predict the solubility of gases in aqueous solutions, high accuracy experimental data are always necessary to validate or improve these predictive tools. Available experimental data in the literature for solubility of CO_2 in mixed salt aqueous solutions were mostly measured at pressures less than 20 MPa. Therefore, additional measurements would be essential to validate models prediction at higher pressures.

In this study, experimental investigations were conducted to measure the solubility of CO_2 in a mixed salts aqueous solution at different isotherms in the temperature range of (300 to 424) K and a pressure up to 41 MPa. Moreover, the solubility of CO_2 in deionised water at the same range of pressure and temperature were determined to check the validity of results obtained in this work. The experimental results were then compared with predictions of the sCPA-EoS [1] and Duan model [2].

2. Literature review

Experimental results for solubility of carbon dioxide in deionised water are plentiful in the literature. Solubility measurement in NaCl aqueous solution are also widely available in the literature. However, experimental results for mixed salt aqueous solutions are scarce. A list of the experimental data available in the literature for measurement of CO_2 solubility in deionised water, NaCl aqueous solutions and mixed salts aqueous solutions are tabulated in **Table 1** to **Table 3**. As shown in these tables most of the literature data for CO_2 solubilities in the single

and mixed salts solutions were measured at low pressure condition. Therefore, further measurements at high pressure would be very useful to fill the gap in the literature data

Table 1. Experimental data available in the literature for CO_2 solubility in deionised water.

Temperature/ K	Pressure / MPa	Aqueous phase	Reference
293.15 – 303.15	0.5 – 3	Deionised Water	[3]
273.15 – 373.15	1 – 9	Deionised Water	[4]
323 – 373	0.25 – 7.1	Deionised Water	[5]
285 – 313	0.25 – 5.07	Deionised Water	[6]
283-303	0.1–2	Deionised Water	[7]
473–523	9.8–49	Deionised Water	[8]
323–533	20–200	Deionised Water	[9]
383–533	10–150	Deionised Water	[10]
303–353	1–3.9	Deionised Water	[11]
323–473	0.1–5.4	Deionised Water	[12]
323–373	10–80	Deionised Water	[13]
288–366	0.7–20.3	Deionised Water	[14]
283–343	1.0–16	Deionised Water	[15]
323.2	Up to 20	Deionised Water	[16]
244.82-298.15	0.69-13.79	Deionised Water	[17]
323–348	10.1–15.2	Deionised Water	[18]
343-421	Up to 20	Deionised Water	[19]
288.15-313.15	6–25	Deionised Water	[20]
313.15-383.15	1-34.48	Deionised Water	[21]
278–293	6.4–29.5	Deionised Water	[22]
274-278	0.89-2.09	Deionised Water	[23]
344	10–100	Deionised Water	[24]
298	2.1–7.7	Deionised Water	[25]
294	10–60.0	Deionised Water	[26]
277–283	2–4.2	Deionised Water	[27]
274–288	0.1–2.2	Deionised Water	[28]
298	7.5–30.0	Deionised Water	[29]
274–351	0.2–9	Deionised Water	[30]
278–318	0.5–8	Deionised Water	[31]
298.15-448.15	Up to 18	Deionised Water	[32]
283-363	Up to 13	Deionised Water	[33]

Table 2. Experimental data available in the literature for CO_2 solubility in single salt-NaCl solutions.

Temperature/ K	Pressure / MPa	Aqueous phase	Reference
273–323	0.101–0.114	NaCl solution	[34]
303–523	4–12.6	NaCl solution	[35]

Temperature/ K	Pressure / MPa	Aqueous phase	Reference
353–471	2–10.2	NaCl solution	[36]
313.15-433.15	Up to 10	NaCl solution	[37]
278–338	0.049–0.084	NaCl solution	[38]
313–393	0.7 -9.2	NaCl solution	[39]
323.1-373.1	Up to 20	NaCl solution	[40]
323.15-423.15	Up to 15	NaCl solution	[41]
323.15-423.15	Up to 20	NaCl solution	[42]
323.15-423.15	Up to 18	NaCl solution	[43]
423–523	10–140	NaCl solution	[44]
303–333	10–20.0	NaCl solution	[45]
323-413	5-40	NaCl solution	[46]

Table 3. Experimental data available in the literature for CO_2 solubility in mixed salts aqueous solutions.

Temperature / K	Pressure / MPa	Aqueous phase	Reference
308-408	Up to 40	Na^+, Ca^{2+}, Mg^{2+}, Cl^-, HCO_3^-, Fe^{2+}, SO_4^{2-}	[47, 48]
308-328	Up to 16	$NaCl + KCl + CaCl_2$	[49]
308-424	Up to 40	$CaCl_2$+ $MgCl_2$	[50]
268-298	1-4.5	$NaCl+MgCl_2+MgSO_4+CaCl_2+KCl+NaHCO_3+NaBr$	[51]
298.15	0.1	$NaCl+NaNO_3+MgCl_2+MgSO_4+CaCl_2+KCl+KNO_3+NH_4Cl+(NH_4)_2SO_4+Na_2SO_4+K_2SO_4+NaHCO_3+Mg(NO_3)_2+MgSO_4+CaCl_2+Ca(NO_3)_2+BaCl_2+AlCl_3+Al_2(SO_4)_3$	[52]
332	29	Ca^{2+}, Mg^{2+}, Na^+, K^+, Fe^{2+}, Cl^-, SO_4^{2-}	[53]

3. Material and Methods

3.1 Materials

In this work, pure CO_2 (0.99995 mole fraction), supplied by Air Products, was used to measure the solubility of CO_2 in deionised water and an aqueous solution of different salts. Properties of the aqueous solution used for the second set of experiments are described in **Table 4**.

Table 4. Properties of the salts used in the aqueous solution.

Salt	CAS Number	wt% in Aqueous Phase	Minimum Purity (%)	Analytical Method	Supplier
NaCl	4647-14-5	7.013	99.5	None	Fisher Scientific
$CaCl_2$	10043-52-4	0.737	99.0	None	Fisher Scientific
$MgCl_2$	7786-30-3	0.087	99.5	None	Fisher Scientific
KCl	7447-40-7	0.066	99.7	None	Fisher Scientific
$SrCl_2$	10476-85-4	0.059	99.0	None	Sigma Aldrich
$BaCl_2$	10361-37-2	0.036	99.0	None	Sigma Aldrich

3.2 Methods

3.2.1 Experimental setup

The setup used in this work is schematically presented in **Figure 1**. In this setup, a pneumatic rocking system is used to provide mixing of CO_2-aqueous phase system ensuring thermodynamic equilibrium. The measurement cell is mounted on an adjustable rotary axis of the rocking system. The rotation degree of the rotary axis and the time interval between each rotation is adjustable. A 300 ml titanium cylindrical high-pressure vessel, manufactured by Proserv, is used as the measurement cell. This cell can work at pressures up to 68 MPa and at temperatures from 203.15 to 423.15 K. The measurement cell is surrounded by a heating jacket connected to a Heating Circulator Bath (Julabo MA-4) to control system temperature. The jacket and pipework are insulated to help maintain a constant temperature. A calibrated Platinum-Resistance thermometer (PRT) is mounted on the body of the heating jacket to measure the cell temperature. As the temperature probe is not located inside the measurement cell, a temperature calibration is carried out using a Prema calibrator in the temperature range of 273.15 to 423.15 K to correct the fluid temperature inside the measurement cell based on the measured temperature of the heating jacket. A precise pressure transducer (Quartzdyne QS10K-B, pressure range 0-207 MPa) is used to measure system pressure during the measurements. This transducer calibrated regularly using a Budenberg deadweight tester.

To measure the solubility of CO_2 in the solution at the specified temperature and pressure, a gasometer (manufactured by VINCI TECHNOLOGIES) is used in this work. The utilised gasometer is capable of retaining a maximum capacity of 4000 cm^3, with a volume and temperature resolution of 0.1 cm^3 and 0.1 K, respectively. Moreover, an Erlenmeyer flask is used for sampling and gas-liquid separation purpose. While sampling, to maintain thermodynamic equilibrium in the measurement cell a bottle of pure CO_2 with an initial pressure of 5 MPa is employed to stabilise pressure inside the measurement cell by injection of pure CO_2. In the case of measurements with a required pressure more than 5 MPa, a booster (Spragu Products-Model: S86JN100) is used to increase injection pressure up to 41 MPa. Furthermore, a Novasina Pro-Labmaster-aw (Novasina AS, Switzerland) is used to measure water activity of samples after each measurement.

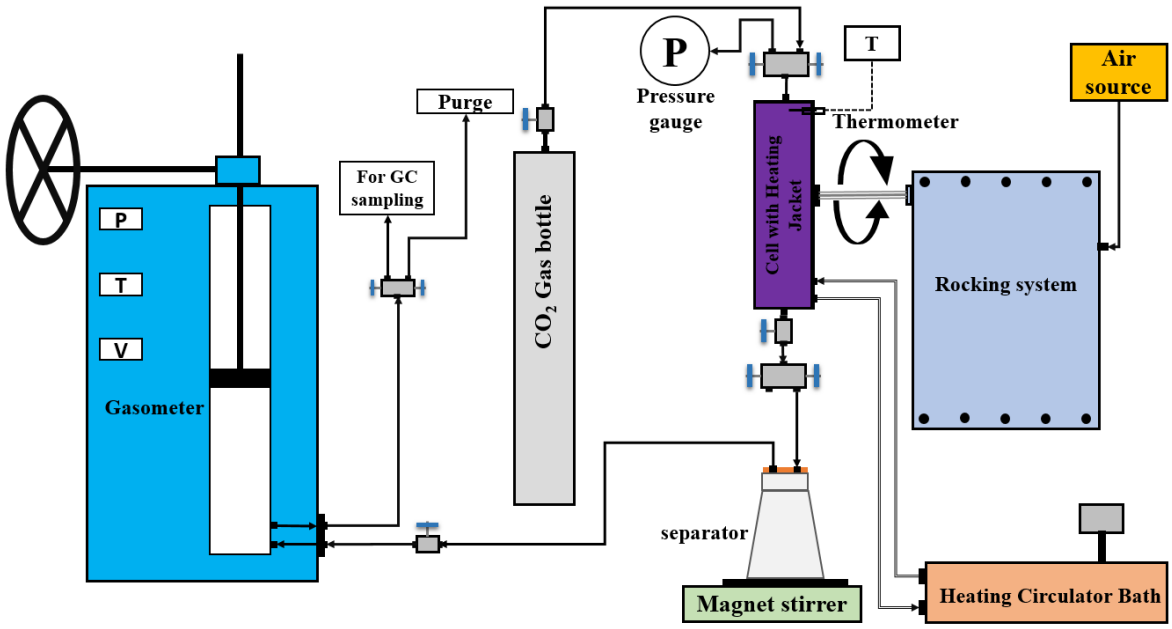

Figure 1. Schematic diagram of the solubility measurement setup

3.2.2 Measurement Procedure

For experimental measurement of CO_2 solubility in different aqueous solutions, the following steps were carried out;

A. Sample preparation: Firstly, the measurement cell was washed, dried and locked in a vertical position. The cell was filled with 230-250 ml of the aqueous solution, following which the top cap of the cell was attached. Then, the air was vacuumed and the heating system was set to achieve the desired temperature. Once the temperature became stable, pure carbon dioxide was injected into the measurement cell (from bottom) to set system pressure to desired value. Then, the rocking cell was initialized and mixing was continued (at least for 30 minutes) until stable pressure and temperature were observed, ensuring equilibrium in the system.

B. Sampling: Before starting the sampling procedure, the Erlenmeyer flask weighted, (M_i), and then connected to the bottom of the measurement cell while it was in a vertical position as shown in **Figure 1**. Before commencing the sampling, the drainage valve of the gasometer was closed, and initial volume (V_i) and pressure (P_g) of the gasometer as well as equilibrium pressure and temperature of the mixture inside the measurement cell, (P, T), were recorded to be used for further calculations. Then, the bottom valve of the measurement cell was opened very slightly to prevent any sudden pressure drop that disrupts the equilibrium condition in the measurement cell. At the same time, pure CO_2 from the gas bottle was injected into the top of the measurement cell to maintain system pressure at equilibrium pressure (P). In all the

measurements, the system pressure was controlled manually to ensure not more than 10 psi (0.07MPa) change in the pressure of the mixture inside the measurement cell. Following the drainage of sample into the flask, the separated gas was transferred to the gasometer and pressure in the gasometer chamber was increased due to the further separation of gas from the liquid sample. For accuracy purpose, sampling was continued until enough volume of gas (at least 400 ml) was collected in the gasometer. Because the maximum allowable operating pressure of the gas inside the gasometer chamber was 20 psia (0.14 MPa), the gas pressure inside the gasometer was regularly controlled by changing the chamber volume employing the rotary crank. When enough sample was collected, the flask was disconnected and left on the magnetic stirrer while it was connected to the gasometer. The liquid sample in the flask was then mixed for 30 minutes at room temperature to separate the gas from the liquid sample and ensure equilibrium in the sample. Then, using the rotary crank, gasometer volume was adjusted to set the gasometer pressure to the same pressure observed at the beginning of the test (P_g), and then, the final volume (V_f) and temperature (T_f) of the gas in the gasometer were recorded. Also, the mass of the flask including the solution inside was measured (M_f).. Finally, the water activity of the sample was measured to ensure the overall composition of the aqueous phase has not changed during sampling.

3.2.3 Solubility Calculations

In addition to the experimental part, further calculations were required to obtain the dissolved amount of CO_2 in the aqueous solution.

The total volume of the gas in the sample taken from the measurement cell was in two parts: first, the gas separated from the liquid sample which was collected in the gasometer, (X_A), and second, the gas remained dissolved in the liquid sample in the Erlenmeyer, (X_A). To calculate each part, following calculations were conducted;

A. Separated gas from liquid sample (X_A)

Before starting the measurement, the total volume of sampling system (Erlenmeyer (V_{Er}) and gasometer) was defined as:

$$V_1 = V_i + V_{Er} \qquad \text{eq. (1)}$$

In this equation, V_1, V_i and V_{Er} stand for the initial total volume of the sampling system, the initial volume of the gasometer and the Erlenmeyer volume, respectively. At the end of the measurement, a liquid sample (with the volume of V_L) was collected in the Erlenmeyer flask,

and the gasometer volume was changed from (V_i) to (V_f) due to the separation of the gas from the liquid sample. Therefore, the total volume of the gas in the system at the end of the experiment, (V_2), was found to be:

$$\boldsymbol{V_2 = V_f + (V_{Er} - V_L)} \qquad \text{eq. (2)}$$

Therefore, the total volume of the gas separated from the liquid sample (V_G) was calculated as:

$$V_G = V_2 - V_1 = V_f - V_i - V_L \qquad \text{eq. (3)}$$

Substituting the liquid volume with mass using the measured mass of the flask before (M_i) and at the of experiment (M_f) gives;

$$V_G = V_f - V_i - \frac{M_L}{\rho_L} = V_f - V_i - \frac{(M_f - M_i)}{\rho_L} \qquad \text{eq. (4)}$$

To calculate the density of the aqueous phase (ρ_L), the IAWPS EoS[54] was used when the aqueous phase was deionised water. Moreover, in case of aqueous phase containing dissolved salts the following correlation suggested by Lewis & Perkin [55] was used to calculate aqueous phase density:

$$\rho_{sw}(\frac{kg}{m^3}) = (a_1 + a_2 t + a_3 t^2 + a_4 t^3 + a_5 t^4) - (b_1 S + b_2 St + b_3 t^2 S + b_4 t^3 S + b_5 S^2 t^2) \qquad \text{eq. (5)}$$

In this equation, temperature and salinity of the brine are represented by ***t*** and ***S***, respectively. The required coefficients and range of validity for this equation are described in **Table 5**.

Table 5. Coefficients and validity range for Lewis& Perkin correlation.

Equation Coefficients		Range of validity
$a_1 = 9.999 \times 10^2$	$b_1 = 8.020 \times 10^2$	$0 < t < 180$℃
$a_2 = 2.034 \times 10^{-2}$	$b_2 = -2.001$	$0 < S < 0.16\ \frac{kg}{kg}$
$a_3 = -6.162 \times 10^{-3}$	$b_3 = 1.677 \times 10^{-2}$	Accuracy: $\pm 0.1\%$
$a_4 = 2.261 \times 10^{-5}$	$b_4 = -3.060 \times 10^{-5}$	
$a_5 = -4.657 \times 10^{-8}$	$b_5 = -1.613 \times 10^{-5}$	

Finally, CO_2 density was used to calculate total moles of CO_2 separated from the liquid sample using the below equation;

$$X_A = (V_f - V_i - \frac{(M_f - M_i)}{\rho_L}) \times \rho_{CO_2} \qquad \text{eq. (6)}$$

The value of CO_2 density used in this equation was calculated using the Span &Wagner EoS [56] at temperature and pressure of the gas in the gasometer condition (T_f, P_g).

B. Dissolved gas in the liquid sample (X_B)

The solubility of CO_2 in the liquid sample in the Erlenmeyer at laboratory temperature (295.15 K) and atmospheric pressure (14.5 psia), was taken from the NIST Standard Reference Database [57] . As a result, the total number of CO_2 moles dissolved in the liquid sample (X_B) was found employing the below formula;

$$X_B = \frac{x_{CO_2}}{1 - x_{CO_2}} \times \left[\frac{(M_f - M_i) \times F_w}{MW_W} + \frac{(M_f - M_i) \times (1 - F_w)}{MW_{salt}}\right] \qquad \text{eq. (7)}$$

In this equation x_{CO2}, MW and F_W stand for equilibrium molar composition of CO_2 in aqueous solution, fluids molecular weight and weight fraction of water in the aqueous solution, respectively. Usually, gas solubility is reported based on the mole fraction of gas dissolved in water. Therefore, for systems with an aqueous phase containing salts, the weight fraction of water (F_W) was used in calculations to convert brine mass to water mass. Also, for an aqueous phase containing more than one salt (S1, S2, etc.), the above equation can be rewritten as;

$$X_B = \frac{x_{CO_2}}{1 - x_{CO_2}} \times \left[\frac{(M_f - M_i) \times F_w}{MW_W} + \frac{(M_f - M_i) \times F_{s1})}{MW_{s1}} + \frac{(M_f - M_i) \times F_{s2})}{MW_{s2}} + \cdots\right] \qquad \text{eq. (8)}$$

Finally, the total solubility of CO_2 in water was found by dividing the total number of CO_2 moles by the total number of CO_2 and water moles.

$$X_{CO_2} = \frac{X_A + X_B}{X_A + X_B + \frac{(M_f - M_i) \times F_w}{MW_W}} \qquad \text{eq. (9)}$$

4. Thermodynamic Modelling

A detailed description of the original thermodynamic model used in this work can be found elsewhere [58-60]. The thermodynamic model is based on the uniformity of fugacity of each component throughout all the phases. The CPA-EoS was used to determine the component fugacities in fluid phases. To take into account the effect of salts on the phase equilibria, the fugacity of non-electrolyte compound is calculated by combining the equation of state with the Debye-Hückel electrostatic contribution.

$$ln\varphi_i = ln\varphi_i^{EoS} + ln\gamma_i^{EL} \qquad \text{eq. (10)}$$

where N is the number of non-electrolyte components, ϕ_i is the fugacity coefficient of component i, ϕ_i^{EoS} is the fugacity coefficient of component i calculated by CPA, neglecting the electrostatic effect, and γ_i^{EL} is the contribution of the electrostatic term.

5. Result and Discussion

5.1 Solubility of CO_2 in Deionised Water

In this study, the solubility of CO_2 in deionised water was measured at 300.95 K, 307.79 K, 322.62 K, 373.39 K and 423.48 K and pressure up to 41 MPa. The experimental results were compared with the prediction of the sCPA-EoS and Duan model and the average absolute deviations (%AAD)* were calculated. Moreover, uncertainties of the measurements were calculated employing the procedure detailed in **APPENDIX**. The measured solubilities of CO_2 in deionised water for each isotherm at different pressures, deviations of results from the predictive models and uncertainty of the measurements (with 95% level of confidence, k=2) are tabulated in **Table 6**. Moreover, measured data points, literature data and predictions of the sCPA-EoS and the Duan model are shown in **Figure 2** to **Figure 6**.

Although many experimental results are available in the literature for the solubility of CO_2 in deionised water, a gap in the literature data was observed in the near-critical region of pure CO_2. The measured solubilities in this work can be used to fill this gap. Furthermore, as depicted in **Figure 3** to **Figure 6**, comparison of the measured data in this study with extensive data available in literature proves the validity of the measured results and methods used in this study.

As it can be seen in **Table 6**, at all isotherms deviations of the experimental results from the predictive models decreased as pressure increased. Also, in comparison with the sCPA-EoS, smaller deviations were observed when the Duan model was used.

Furthermore, comparison of the available experimental results found in the literature, the data measured in this work and predictions of the models used in this work confirmed the limits of the sCPA-EoS in the prediction of the CO_2 solubilities in deionised water, especially at lower pressures.

---

* $AAD\% = \frac{100}{n} \times \sum_{i=1}^{n} \frac{\left|X_i^{EXP} - X_i^{model}\right|}{X_i^{EXP}}$

All measured solubilities and the models predictions are presented in **Figure 7**. As shown in this figure, in the first four isotherms solubility of the gas decreased as temperature increased. It was because of the higher kinetic energy of the aqueous phase molecules at a higher temperature that broke the intermolecular bonds of the solution and helped the gas molecules to escape from solution. However, in the last isotherm (423.48 K) at pressures more than the intermediate pressure (20 MPa), the solubility of the gas increased to values more than the observed solubilities at lower temperatures.

As expected, the effect of increasing pressure was to increase the solubility. However, effects of pressure on solubility of the gas decreased as pressure increased. As a result of pressure increase, the number of gas molecules per unit of volume was increased. Therefore, at higher pressures, more gas molecules were in contact with the liquid surface, and the solubility of gas increased.

Table 6. Measured CO_2 solubility in deionised water at different isotherms.

	Pressure*	x_{CO2}	Expanded Uncertainty	Deviations (%) ***	
	MPa	(mole fraction)	(k=2)	sCPA-EoS	Duan model
T =300.95 K**	2.071	0.01099	0.00011	16.0	7.1
	4.782	0.02032	0.00017	5.7	4.5
	7.837	0.02335	0.00023	-5.2	-1.4
	19.445	0.02696	0.00028	-2.9	1.8
	34.753	0.02960	0.00034	-2.8	0.6
		%AAD		**6.53**	**3.08**
T=307.79 K**	1.292	0.00601	0.00011	14.3	3.8
	1.310	0.00601	0.00011	13.2	2.6
	2.243	0.00974	0.00012	10.6	3.0
	3.380	0.01384	0.00014	8.7	4.5
	4.594	0.01704	0.00017	4.0	2.8
	5.543	0.01931	0.00017	2.2	3.1
	7.143	0.02228	0.00022	0.4	3.4
	12.231	0.02414	0.00025	-3.5	3.4
	19.236	0.02589	0.00027	-3.8	3.6
		%AAD		**6.75**	**3.36**
T=322.62 K**	2.991	0.00961	0.00011	11.4	4.0
	4.778	0.01279	0.00012	0.0	-4.1
	5.486	0.01493	0.00013	4.3	1.8
	8.667	0.01959	0.00020	1.1	2.4
	20.727	0.02394	0.00025	-2.8	4.2
	40.349	0.02708	0.00031	-4.6	2.3
		%AAD		**4.04**	**3.12**
T=373.39 K**	3.515	0.00697	0.00011	24.41	13.21
	7.941	0.01286	0.00013	15.57	8.01
	19.34	0.02112	0.00022	8.69	8.33
	42.077	0.02578	0.00025	-1.08	2.01
		%AAD		**12.44**	**7.89**
T=423.48 K**	2.631	0.00327	0.00011	14.3	-3.8
	5.109	0.00665	0.00011	12.4	-3.4
	9.772	0.01170	0.00012	7.1	-5.2
	19.549	0.02063	0.00019	8.3	1.9
	40.690	0.02839	0.00032	-2.6	-3.2

* $U_c(P)$ = 0.068 MPa, ** $U_c(T)$ = 0.17 K, *** Deviation (%)$=100 \times \frac{(x^{Exp}-x^{model})}{x^{Exp}}$

	Pressure*	x_{CO2}	Expanded Uncertainty	Deviations (%) ***	
	MPa	(mole fraction)	(k=2)	sCPA-EoS	Duan model
		%AAD		8.93	3.50

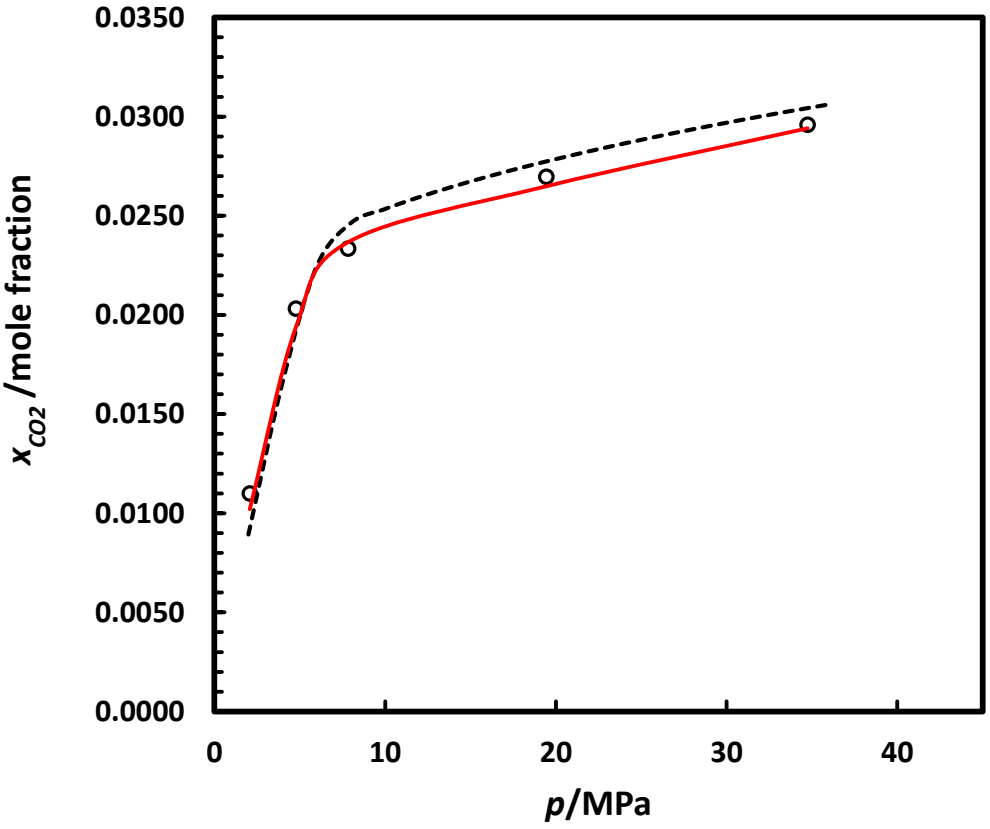

Figure 2. Mole fraction of CO_2 dissolved in deionised water at T= 300.95 K. This work (O), the Duan model (—), the sCPA-EoS (- - -).

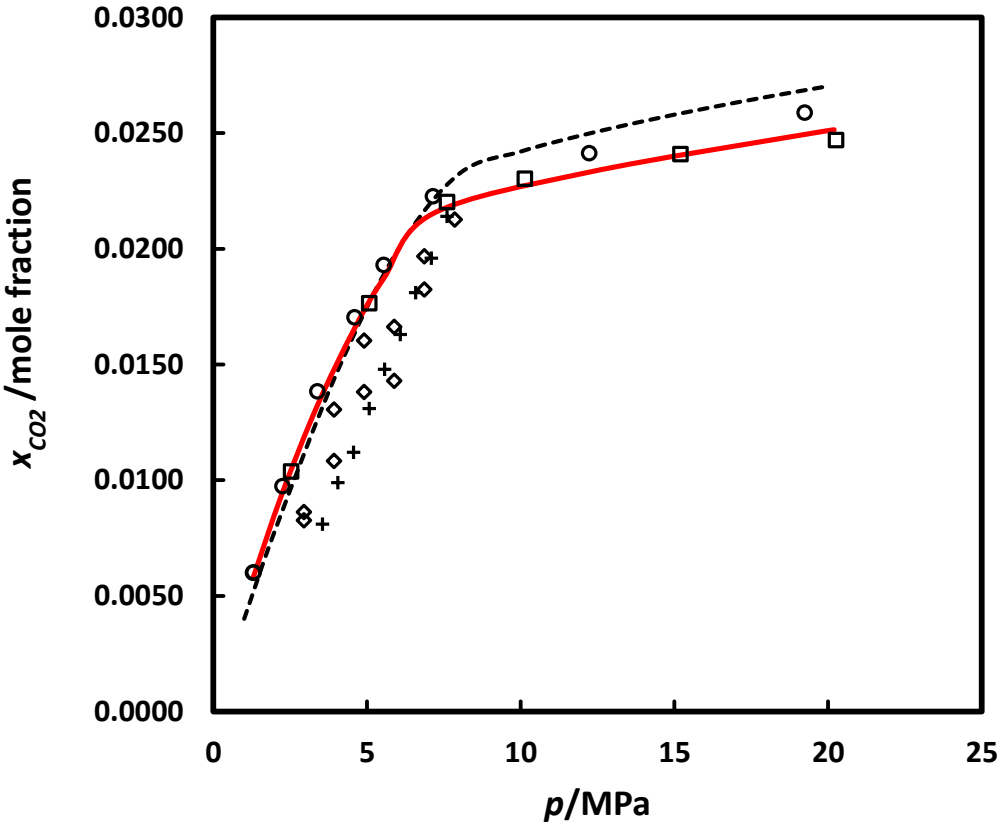

Figure 3. Mole fraction of CO_2 dissolved in deionised water at T= 307.79 K.

This work (O), Models: the Duan model (—), the sCPA-EoS (- - -), literature data: Sander [24] (♦), Vilcu et al. [61] (✚), Wiebe et al. [6] (□).

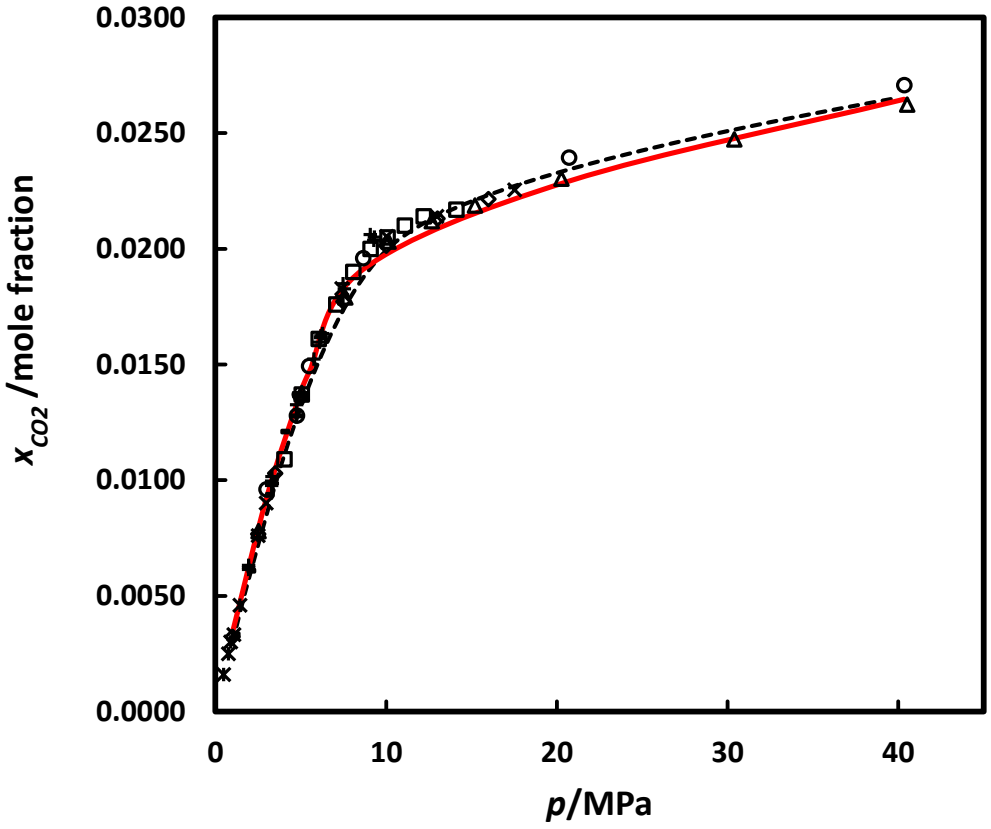

Figure 4. Mole fraction of CO_2 dissolved in deionised water.

This work at T= 322.57 K. (O), Models: the Duan model (—), the sCPA-EoS (- - -), literature data at 323.15 K: Oleinik [15] (♦), Hou et al. [32] (✖), Zel'vinskii [4] (✚), Wiebe et al. [6] (▲), Matous et al. [11] (-), Zawisza et al. [12](✱), Bamberger et al. [62] (□), Malinin et al. [63] (–).

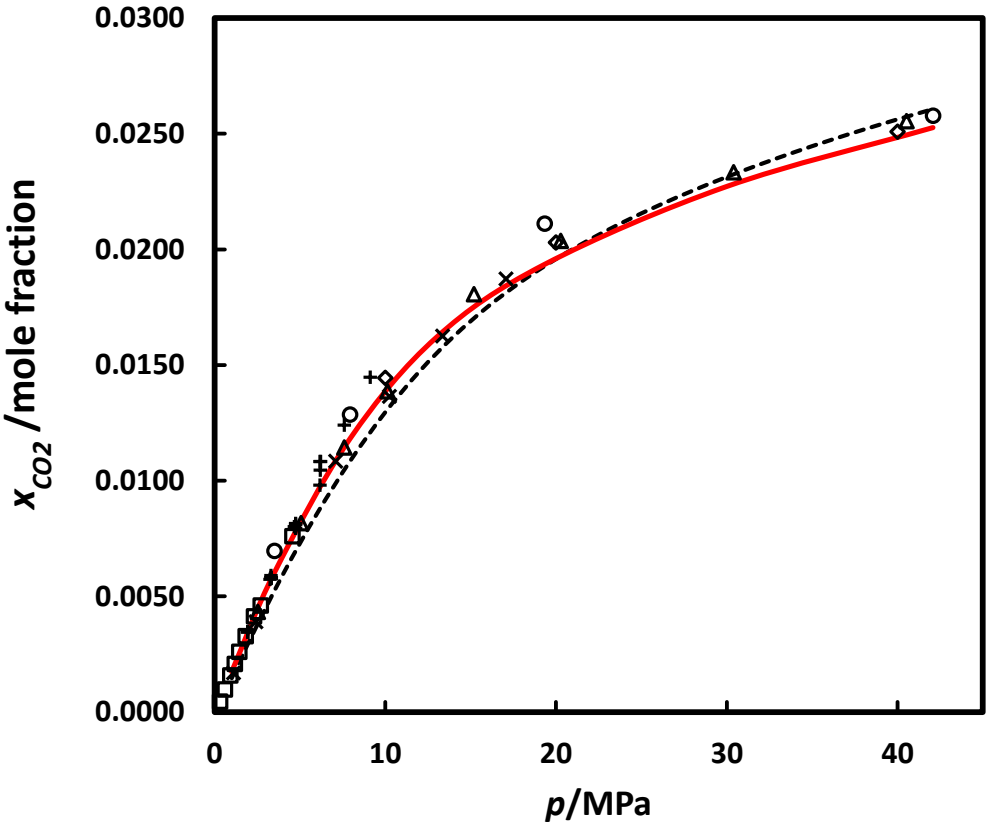

Figure 5. Mole fraction of CO_2 dissolved in deionised water at T=373.39 K.

This work (O), Models: the Duan model (—), the sCPA-EoS (- - -), literature data: Shagiakhmetov et al. [13](♦), Hou et al. [32] (✖), Zel'vinskii [4] (✚), Wiebe et al. [6] (▲), Zawisza et al. [12] (▫).

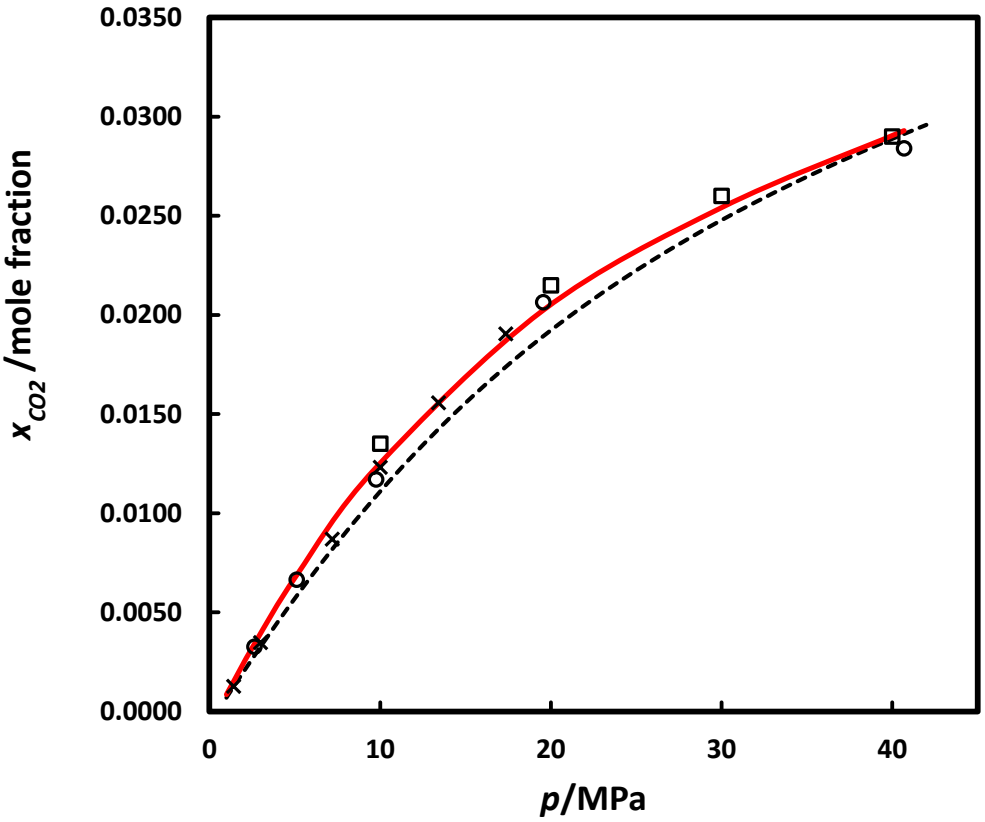

Figure 6. Mole fraction of CO_2 dissolved in deionised water at T=423.48 K.

This work (O), Models: the Duan model (—), the sCPA-EoS (- - -), literature data: Takenouchi et al. [10] (□), Hou et al. [32] (×).

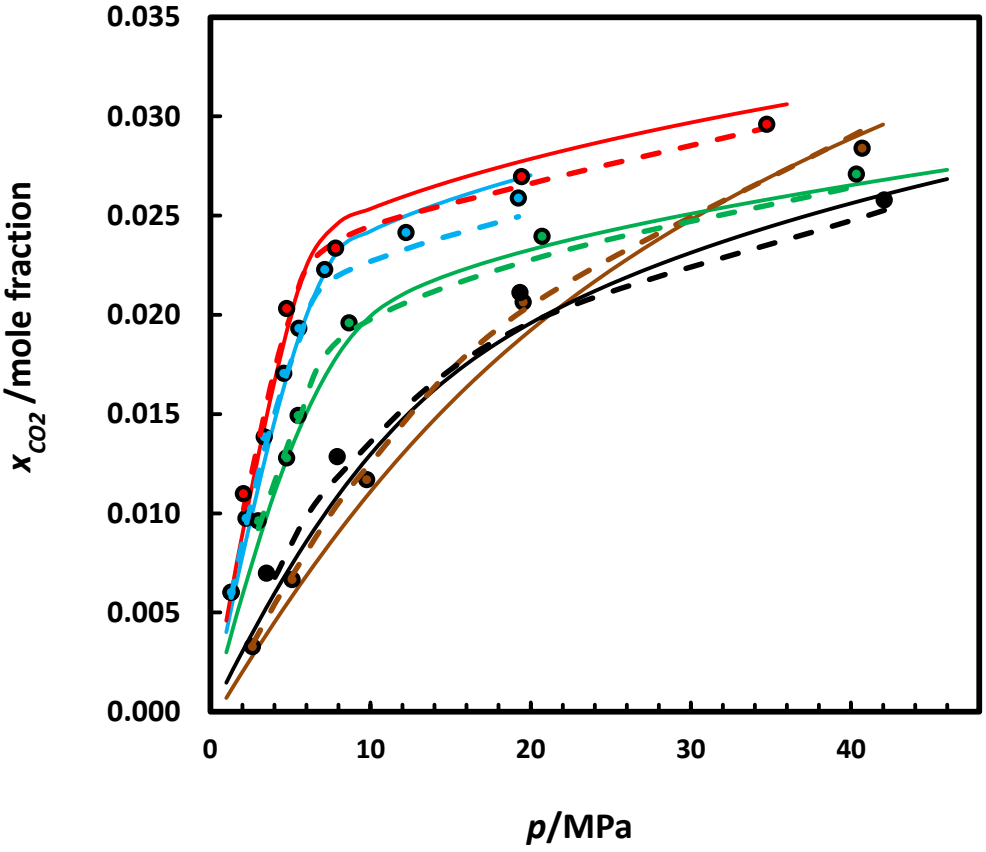

Figure 7. Mole fraction of CO_2 dissolved in deionised water at different isotherms.

This work (O), Models: the Duan model (—), the sCPA-EoS (– – –),

T=300.95 K, 307.79 K, 322.57 K, 373.39 K, 423.48 K.

5.2 Solubility of CO_2 in the mixed salts aqueous solution

In the second set of experiments of this study, measurements were carried out to obtain the solubility of CO_2 in the mixed salts aqueous solution. These measurements were carried out at 303.16 K, 323.20 K, 373.19 K and 423.19 K and up to 39 MPa. Also, the measured water activities for fresh aqueous phase and all the experimental samples were found to be 0.953±0.002, which was in agreement with the predictions of the sCPA-EOS. Deviations of the experimental results compared with the prediction of the sCPA-EoS and the Duan model, as well as uncertainties of the measurements are reported in **Table 7**. For each model, two

solubilities were calculated using two assumptions; in the first calculation, the aqueous solution was assumed to be a mixture of water and NaCl (single salt). In the second calculation, different salts in the aqueous solution were considered (mixed salts). Assuming the brine as a single salt mixture, the average absolute deviation (%AAD) of the measured data points in comparison with the sCPA-EoS and the Duan model were found to be 4.71% and 3.00%, respectively. Using the second assumption, brine as a mixed salts, did not change the calculated %AADs notably. In this case, the %AAD of the measured results in comparison with the sCPA-EoS and the Duan model were found to be 4.71% and 3.05%, respectively. The experimental results and model predictions for both cases (single salt/mixed salts) are depicted in **Figure 8** and **Figure 9**. Individual figures of the results for each isotherm can be found in the **Supporting Information**.

Similar to measured solubilities in deionised water, larger deviations of the results from the predictive models were observed when measurements were conducted at low pressure condition. Also, in comparison to the measured solubilities of CO_2 in deionised water, less gas was dissolved in the brine which can be explained using the salting-out effect. This effect can be shown using the Setschenow constant (k_s) in the below equation [64]:

$$\log\left(\frac{S_0}{S}\right) = k_s C_s \qquad \text{eq. (11)}$$

Where S_0 and S are the solute's solubility in deionised water and brine, respectively. Also, k_s is the Setschenow constant, and C_s represents the concentration of salt in the brine. Using this formula Setschenow constant was found for each data point. For all the data points the values of k_s were almost similar and the average value was found to be 0.08694 kg.mole^{-1}.

Table 7. Measured CO_2 solubility in the mixed salts aqueous phase at different isotherms

	Pressure*	x_{CO2}	Expanded Uncertainty	Deviations (%)***			
				Single salt (NaCl)		Mixed salts (all salts)	
	MPa	(mole fraction)	(k=2)	sCPA-EoS	Duan model	sCPA-EoS	Duan model
T=303.16 K**	1.625	0.00527	0.00011	-0.77	-10.29	-0.56	-12.15
	6.612	0.01649	0.00019	-0.32	0.26	-0.11	-1.46
	8.675	0.01804	0.00024	2.35	5.02	2.55	3.38
	20.519	0.01913	0.00028	-3.09	-0.49	-2.87	-2.21
	35.386	0.02096	0.00031	-2.17	-2.33	-1.94	-4.02
	%AAD			**1.74**	**3.68**	**1.61**	**4.64**
T=323.20 K**	1.763	0.00443	0.00011	10.88	2.02	10.95	0.48
	6.257	0.01192	0.00011	2.31	0.72	2.36	-0.89
	10.719	0.01540	0.00018	-0.05	1.04	0.02	-0.57
	18.172	0.01708	0.00023	-1.47	2.88	-1.40	1.30
	38.860	0.01975	0.00029	-1.90	0.80	-1.82	-0.75
	%AAD			**3.32**	**1.49**	**3.31**	**0.80**
T=373.19 K**	1.929	0.00232	0.00011	18.33	6.47	18.33	6.47
	8.172	0.00860	0.00008	6.68	0.56	6.65	-0.96
	22.895	0.01561	0.00019	3.35	3.95	3.32	2.46
	38.808	0.01877	0.00026	-0.70	1.14	-0.73	-0.37
	%AAD			**7.27**	**3.03**	**7.26**	**2.57**
T=423.19 K**	2.415	0.00244	0.00011	16.48	3.31	16.68	1.92
	5.434	0.00498	0.00006	1.22	-10.82	1.48	-12.50
	9.253	0.00879	0.00007	8.10	-0.18	8.35	-1.75
	24.335	0.01720	0.00018	4.21	2.81	4.49	1.22
	36.949	0.01999	0.00021	-2.62	-19.3	-2.30	-3.63
	%AAD			**6.53**	**3.81**	**6.66**	**4.20**

* U_c (P) = 0.068 MPa, ** U_c (T) = 0.17 K, *** Deviation (%)$=100 \times \frac{(x^{Exp}-x^{model})}{x^{Exp}}$

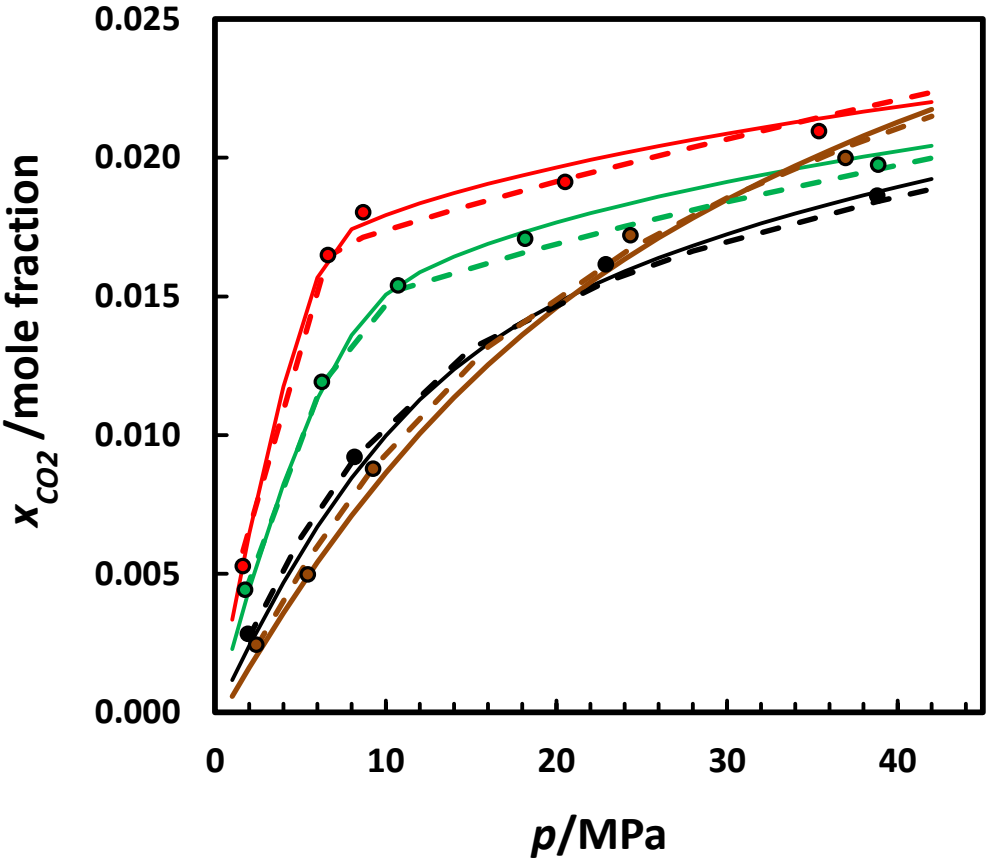

Figure 8. Mole fraction of CO_2 dissolved in the mixed salts aqueous solution at different isotherms.

This work (O), Models (single salt): the Duan model (—), the sCPA-EoS (– – –).

T= 303.16 K, 323.20 K, 373.19 K, 423.19 K.

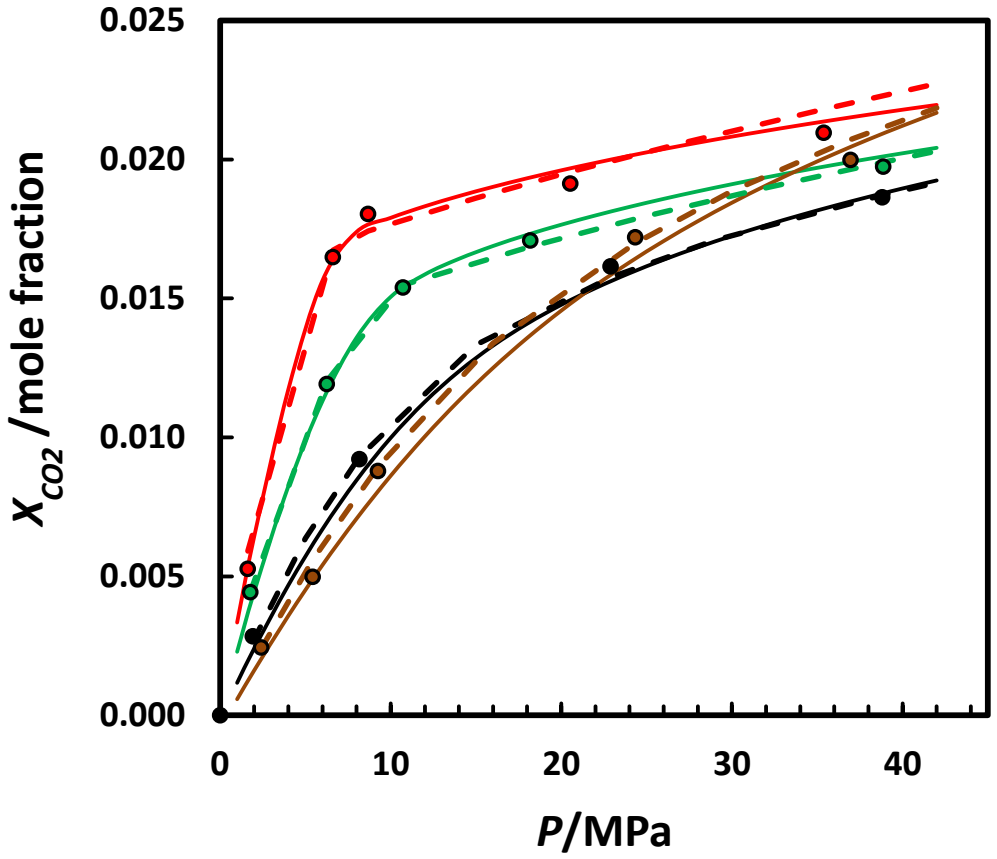

Figure 9. Mole fraction of CO_2 dissolved in the mixed salts aqueous solution at different isotherms. This work (O), Models (mixed salts): the Duan model (—), the sCPA-EoS (– – –). T= 303.16 K, 323.20 K, 373.19 K, 423.19 K.

Similar to the observed results for solubility of CO_2 in deionised water, increasing temperature to 373 K caused a decrease in solubility of CO_2 in the mixed salts aqueous solution. Also, for the isotherm with higher temperature, an increase in solubility was observed when system pressure was more than 20 MPa. Moreover, in comparison with deionised water, the solubility of CO_2 in the mixed salts aqueous solution was reduced as a consequence of salting out effect [65, 66]. As an example, at 373.19 K an average reduction of about 17% in CO_2 solubility was found when solubilities in mixed salt solution were compared with deionised water.

6. Conclusion

In this work, the solubility of CO_2 in deionised water was measured in a pressure range up to 41 MPa and for different isotherms up to 423.48 K. first, the solubility of CO_2 in deionised water was measured and compared against the available data in the literature to validate the experimental setup and procedures used in this study. Then, CO_2 solubility in a mixed salt aqueous solutions (salinity: ~ 80000 ppm) was measured in a pressure range up to 39 MPa and for different isotherms up to 423.19 K.

All the measured solubilities were compared against the prediction of the sCPA-EoS and the Duan model. The average absolute deviations (%AAD) of results in comparison with the sCPA-EoS were found to be 7.74% and 4.71% for deionised water and the aqueous solution (single salt-NaCl), respectively. For both cases, deviations were observed mostly at low pressure, confirming limits of sCPA-EoS in solubility prediction at low pressure when tuned over a wide pressure range. Also, when results were compared with the prediction of the Duan model, the calculated average absolute deviations (%AAD) were 4.19% and 3.00% for deionised water and the aqueous solution (single salt-NaCl), respectively. Also, the average uncertainty of the measurements conducted to obtain CO_2 solubility in deionised water and mixed salts aqueous solution were found to be 1.20% and 1.57%, respectively.

7. Appendix-Uncertainties of the measurements

a. Temperature uncertainty: In this setup uncertainty of temperature measurement was calculated according to:

$$U_c(T) = \sqrt{u_{thermometer}{}^2 + u_{calibration}{}^2 + u_{repeatability}{}^2} \quad \text{eq. (A1)}$$

The system and repeatability uncertainties were found to be 0.1 K. Moreover, the calibration function used to convert the measured temperature in the jacket of the cell to the actual temperature in the cell was:

$$T_{Calibrated}(T) = 0.9633\text{T} + 0.9208 \quad \text{eq. (A2)}$$

Therefore, $u_{calibration}$ was obtained according to:

$$u_{calibration} = \left|\frac{dT_{Calibrated}}{dT}\right| . \Delta T \quad \text{eq. (A3)}$$

In this equation, ΔT was equal to 0.1 K and derivative of the calibration function was 0.9633.

As a result $U_c(T)$ was found to be 0.17 K for all points.

b. Pressure uncertainty: similar to the temperature uncertainty, the uncertainty of pressure measurements was calculated according to the following equations:

$$U_c(P) = \sqrt{u_{system}{}^2 + u_{calibration}{}^2 + u_{repeatability}{}^2} \quad \text{eq. (A4)}$$

The high accuracy pressure transducer used in this work was regularly calibrated. Also, $u_{repeatability}$ for this transducer was found to be 0.007 MPa. In this experiment during sampling, system pressure was controlled by injecting the gas to prevent any pressure change more than 10 psi (0.068 MPa) in the system. Therefore, u_{system} for these measurements was found to be 0.068 MPa.

As a result $U_c(P)$ was found to be 0.068 MPa with three digits accuracy for all the measurements.

c. Uncertainty of solubility measurement

In comparison with the previous uncertainty calculations, no calibration uncertainty are required for the sampling part of this experiment. Therefore, the uncertainty of the measurements was calculated using the following equation:

$$\Delta U = \sqrt{u_{Measurement}{}^2 + u_{repeatability}{}^2} \qquad \text{eq. (A5)}$$

Some of the measurements were repeated, and the average standard deviation of the repeated tests was reported as the uncertainty of repeatability. The $u_{repeatability}$ for the experiments conducted in this study was found to be 0.000053.

To calculate the uncertainty of the measurements, the main formula used to calculate the solubility of the gas in water was split into different parts for ease of calculations.

$$x_{CO_2} = \frac{X_A + X_B}{X_A + X_B + \frac{(M_f - M_i) \times F_w}{W_{MW}}} \qquad \text{eq. (A6)}$$

To simplify this equation, Z and R were defined as

$$Z = X_A + X_B \qquad \text{eq. (A7)}$$

$$R = \frac{(M_f - M_i) \times F_w}{W_{MW}} \qquad \text{eq. (A8)}$$

The uncertainties of Z and R were calculated by

$$\Delta Z = \sqrt{(\Delta X_A)^2 + (\Delta X_B)^2} \qquad \text{eq. (A9)}$$

$$\Delta R = \frac{F_w}{W_{MW}} \times \sqrt{(\Delta M_f)^2 + (\Delta M_i)^2} \qquad \text{eq. (A10)}$$

To calculate ΔZ, X_A was split to C1 and C2. Also, uncertainties of volume measurements in the gasometer, mass measurements and density calculations were used to calculate total uncertainty of the measurements. ($\Delta V_f = \Delta V_i = 0.1\, ml$, $\Delta M_f = \Delta M_i = 0.01\, g$, $\Delta \rho_L = 0.001 \rho_L$ and $\Delta \rho_{CO_2} = 0.0005 \rho_{CO_2}$)

$$X_A = (V_f - V_i - \frac{(M_f - M_i)}{\rho_L}) \times \rho_{CO_2} \qquad \text{eq. (A11)}$$

$$C1 = V_f - V_i \Rightarrow \Delta C1 = \sqrt{\left(\Delta V_f\right)^2 + (\Delta V_i)^2} \qquad \text{eq. (A12)}$$

$$C2 = \frac{(M_f - M_i)}{\rho_L} \Rightarrow \frac{\Delta C2}{C2} = \sqrt{\left(\frac{\sqrt{(\Delta M_f)^2 + (\Delta M_i)^2}}{M_f - M_i}\right)^2 + \left(\frac{\Delta \rho_L}{\rho_L}\right)^2} \qquad \text{eq. (A13)}$$

$$\frac{\Delta X_A}{X_A} = \sqrt{\left(\frac{\sqrt{(\Delta C1)^2+(\Delta C2)^2}}{C1-C2}\right)^2 + \left(\frac{\Delta \rho_{CO_2}}{\rho_{CO_2}}\right)^2} \quad \text{eq. (A14)}$$

Also, to calculate the uncertainty of X_B, D1 and D2 were defined for ease of calculations.

$$X_B = \frac{x_{CO_2}}{1-x_{CO_2}} \times \left[\frac{(M_f-M_i)\times F_w}{MW_W} + \frac{(M_f-M_i)\times(1-F_w)}{MW_{NaCl}}\right] \quad \text{eq. (A15)}$$

$$D1 = \frac{x_{CO_2}}{1-x_{CO_2}} \Rightarrow \frac{\Delta D1}{D1} = \sqrt{\left(\frac{\Delta x_{CO_2}}{x_{CO_2}}\right)^2 + \left(\frac{\Delta x_{CO_2}}{1-x_{CO_2}}\right)^2} \quad \text{eq. (A16)}$$

$$D2 = \frac{(M_f-M_i)\times F_w}{MW_W} + \frac{(M_f-M_i)\times(1-F_w)}{MW_{salt}} \Rightarrow \quad \text{eq. (A17)}$$

$$\frac{\Delta D2}{D2} = \frac{F_w}{MW_W}\sqrt{(\Delta M_f)^2 + (\Delta M_i)^2} + \frac{1-F_w}{MW_{salt}}\sqrt{(\Delta M_f)^2 + (\Delta M_i)^2}$$

Finally, the uncertainty of ΔX_B can be obtained using:

$$\frac{\Delta X_B}{X_B} = \sqrt{\left(\frac{\Delta D2}{D2}\right)^2 + \left(\frac{\Delta D1}{D1}\right)^2} \quad \text{eq. (A18)}$$

Finally, using the defined functions, the uncertainty of measurements was found using following equation:

$$u_{measurements} = \Delta X_{CO_2} = X_{CO_2} \times \sqrt{\left(\frac{\Delta Z}{Z}\right)^2 + \left(\frac{\sqrt{(\Delta Z)^2+(\Delta R)^2}}{Z+R}\right)^2} \quad \text{eq. (A19)}$$

The expanded uncertainty of these measurements can be found using the equation below:

$$U_{Expanded} = 2 \times \sqrt{u_{Measurement}{}^2 + u_{repeatability}{}^2} \quad \text{eq. (A20)}$$

Funding

This research did not receive any specific grant from funding agencies in the public, commercial, or not-for-profit sectors.

8. References

[1]. Kontogeorgis, G.M., E.C. Voutsas, I.V. Yakoumis, and D.P. Tassios, *An equation of state for associating fluids.* Industrial & engineering chemistry research, 1996. **35**(11): p. 4310-4318.

[2]. Duan, Z. and R. Sun, *An improved model calculating CO 2 solubility in pure water and aqueous NaCl solutions from 273 to 533 K and from 0 to 2000 bar.* Chemical geology, 2003. **193**(3): p. 257-271.

[3]. Kritschewsky, I., N. Shaworonkoff, and V. Aepelbaum, *Combined solubility of gases in liquids under pressure. I. Solubility of carbon dioxide in water from its mixtures with hydrogen of 20 and 30 C and total pressure of 30 kg/cm2.* Z. Phys. Chem., A, 1935. **175**: p. 232-238.

[4]. Zel'vinskii, Y., *Measurements of carbon dioxide solubility in water.* Zhurn. Khim. Prom, 1937. **14**: p. 1250-1257.

[5]. Wiebe, R. and V. Gaddy, *The solubility in water of carbon dioxide at 50, 75 and 100, at pressures to 700 atmospheres.* Journal of the American Chemical Society, 1939. **61**(2): p. 315-318.

[6]. Wiebe, R. and V. Gaddy, *The solubility of carbon dioxide in water at various temperatures from 12 to 40 and at pressures to 500 atmospheres. Critical phenomena.* Journal of the American Chemical Society, 1940. **62**(4): p. 815-817.

[7]. Bartholomé, E. and H. Friz, *Solubility of CO2 in water.* Chem. Ing. Tech, 1956. **28**: p. 706-708.

[8]. Malinin, S., *The system water-carbon dioxide at high temperatures and pressures.* Geokhimiya, 1959. **3**: p. 292-306.

[9]. Tödheide, K. and E. Franck, *Das Zweiphasengebiet und die kritische Kurve im System Kohlendioxid–Wasser bis zu Drucken von 3500 bar.* Zeitschrift für Physikalische Chemie, 1963. **37**(5_6): p. 387-401.

[10]. Takenouchi, S. and G.C. Kennedy, *The binary system H2O-CO2 at high temperatures and pressures.* American Journal of Science, 1964. **262**(9): p. 1055-1074.

[11]. Matouš, J., J. Šobr, J. Novak, and J. Pick, *Solubility of carbon dioxide in water at pressures up to 40 atm.* Collection of Czechoslovak Chemical Communications, 1969. **34**(12): p. 3982-3985.

[12]. Zawisza, A. and B. Malesinska, *Solubility of carbon dioxide in liquid water and of water in gaseous carbon dioxide in the range 0.2-5 MPa and at temperatures up to 473 K.* Journal of Chemical and Engineering Data, 1981. **26**(4): p. 388-391.

[13]. Shagiakhmetov, R. and A. Tarzimanov, *Measurements of CO2 solubility in water up to 60 MPa.* Deposited Document SPSTL 200khp-D81-1982, 1981.

[14]. Gillespie, P.C. and G.M. Wilson, *Vapor-liquid and liquid-liquid equilibria: water-methane, water-carbon dioxide, water-hydrogen sulfide, water-npentane, water-methane-npentane*. 1982: Gas Processors Association.

[15]. Oleinik, P., *Method of evaluating gases in liquids and volumetric properties of solutions under pressure.* Neftepromyslovoe Delo, 1986.

[16]. Nakayama, T., H. Sagara, K. Arai, and S. Saito, *High pressure liquid・liquid equilibria for the system of water, ethanol and 1, 1-difluoroethane at 323.2 K.* Fluid Phase Equilibria, 1987. **38**(1-2): p. 109-127.

[17]. Song, K.Y. and R. Kobayashi, *Water content of CO2 in equilibrium with liquid water and/or hydrates.* SPE Formation Evaluation, 1987. **2**(04): p. 500-508.

[18]. D'souza, R., J.R. Patrick, and A.S. Teja, *High pressure phase equilibria in the carbon dioxide‐n‐Hexadecane and carbon dioxide—water systems.* The Canadian Journal of Chemical Engineering, 1988. **66**(2): p. 319-323.

[19]. Sako, T., T. Sugeta, N. Nakazawa, T. Okubo, M. Sato, T. Taguchi, and T. Hiaki, *Phase equilibrium study of extraction and concentration of furfural produced in reactor using supercritical carbon dioxide.* Journal of chemical engineering of Japan, 1991. **24**(4): p. 449-455.

[20]. King, M., A. Mubarak, J. Kim, and T. Bott, *The mutual solubilities of water with supercritical and liquid carbon dioxides.* The Journal of Supercritical Fluids, 1992. **5**(4): p. 296-302.

[21]. Jackson, K., L.E. Bowman, and J.L. Fulton, *Water solubility measurements in supercritical fluids and high-pressure liquids using near-infrared spectroscopy.* Analytical Chemistry (Washington), 1995. **67**(14).

[22]. Teng, H., A. Yamasaki, M.-K. Chun, and H. Lee, *Solubility of liquid CO 2 in water at temperatures from 278 K to 293 K and pressures from 6.44 MPa to 29.49 MPa and densities of the corresponding aqueous solutions.* The Journal of Chemical Thermodynamics, 1997. **29**(11): p. 1301-1310.

[23]. Malegaonkar, M.B., P.D. Dholabhai, and P.R. Bishnoi, *Kinetics of carbon dioxide and methane hydrate formation.* The Canadian Journal of Chemical Engineering, 1997. **75**(6): p. 1090-1099.

[24]. Dhima, A., J.-C. de Hemptinne, and J. Jose, *Solubility of hydrocarbons and CO2 mixtures in water under high pressure.* Industrial & engineering chemistry research, 1999. **38**(8): p. 3144-3161.

[25]. Yang, S., I. Yang, Y. Kim, and C. Lee, *Measurement and prediction of phase equilibria for water+ CO 2 in hydrate forming conditions.* Fluid Phase Equilibria, 2000. **175**(1): p. 75-89.

[26]. Rosenbauer, R., J. Bischoff, and T. Koksalan. *An experimental approach to CO2 sequestration in saline aquifers: application to Paradox Valley, CO*. in *AGU Fall Meeting Abstracts*. 2001.

[27]. Servio, P. and P. Englezos, *Effect of temperature and pressure on the solubility of carbon dioxide in water in the presence of gas hydrate.* Fluid Phase Equilibria, 2001. **190**(1): p. 127-134.

[28]. Anderson, G.K., *Solubility of carbon dioxide in water under incipient clathrate formation conditions.* Journal of Chemical & Engineering Data, 2002. **47**(2): p. 219-222.

[29]. Teng, H. and A. Yamasaki, *Pressure-mole fraction phase diagrams for co 2-pure water system under temperatures and pressures corresponding to ocean waters at depth to 3000 M.* Chemical Engineering Communications, 2002. **189**(11): p. 1485-1497.

[30]. Chapoy, A., A. Mohammadi, A. Chareton, B. Tohidi, and D. Richon, *Measurement and modeling of gas solubility and literature review of the properties for the carbon dioxide− water system.* Industrial & engineering chemistry research, 2004. **43**(7): p. 1794-1802.

[31]. Valtz, A., A. Chapoy, C. Coquelet, P. Paricaud, and D. Richon, *Vapour–liquid equilibria in the carbon dioxide–water system, measurement and modelling from 278.2 to 318.2 K.* Fluid phase equilibria, 2004. **226**: p. 333-344.

[32]. Hou, S.-X., G.C. Maitland, and J.M. Trusler, *Measurement and modeling of the phase behavior of the (carbon dioxide+ water) mixture at temperatures from 298.15 K to 448.15 K.* The Journal of Supercritical Fluids, 2013. **73**: p. 87-96.

[33]. Carvalho, P.J., L.M. Pereira, N.P. Gonçalves, A.J. Queimada, and J.A. Coutinho, *Carbon dioxide solubility in aqueous solutions of NaCl: Measurements and modeling with electrolyte equations of state.* Fluid Phase Equilibria, 2015. **388**: p. 100-106.

[34]. Harned, H.S. and R. Davis Jr, *The ionization constant of carbonic acid in water and the solubility of carbon dioxide in water and aqueous salt solutions from 0 to 50.* Journal of the American Chemical Society, 1943. **65**(10): p. 2030-2037.
[35]. Drummond, S.E., *Boiling and mixing of hydrothermal fluids: chemical effects on mineral precipitation*. 1981: Pennsylvania State University.
[36]. Nighswander, J.A., N. Kalogerakis, and A.K. Mehrotra, *Solubilities of carbon dioxide in water and 1 wt% NaCl solution at pressures up to 10 MPa and temperatures from 80 to 200 C.* J. Chem. Eng. Data, 1989. **34**(3): p. 355-360.
[37]. Rumpf, B., H. Nicolaisen, C. Öcal, and G. Maurer, *Solubility of carbon dioxide in aqueous solutions of sodium chloride: experimental results and correlation.* Journal of solution chemistry, 1994. **23**(3): p. 431-448.
[38]. Zheng, D.-Q., T.-M. Guo, and H. Knapp, *Experimental and modeling studies on the solubility of CO2, CHC1F2, CHF3, C2H2F4 and C2H4F2 in water and aqueous NaCl solutions under low pressures.* Fluid Phase Equilibria, 1997. **129**(1-2): p. 197-209.
[39]. Kiepe, J., S. Horstmann, K. Fischer, and J. Gmehling, *Experimental determination and prediction of gas solubility data for CO2+ H2O mixtures containing NaCl or KCl at temperatures between 313 and 393 K and pressures up to 10 MPa.* Industrial & Engineering Chemistry Research, 2002. **41**(17): p. 4393-4398.
[40]. Koschel, D., J.-Y. Coxam, L. Rodier, and V. Majer, *Enthalpy and solubility data of CO 2 in water and NaCl (aq) at conditions of interest for geological sequestration.* Fluid phase equilibria, 2006. **247**(1): p. 107-120.
[41]. Zhao, H., M.V. Fedkin, R.M. Dilmore, and S.N. Lvov, *Carbon dioxide solubility in aqueous solutions of sodium chloride at geological conditions: Experimental results at 323.15, 373.15, and 423.15 K and 150bar and modeling up to 573.15 K and 2000bar.* Geochimica et Cosmochimica Acta, 2015. **149**: p. 165-189.
[42]. Messabeb, H., F.o. Contamine, P. Cézac, J.P. Serin, and E.C. Gaucher, *Experimental Measurement of CO2 Solubility in Aqueous NaCl Solution at Temperature from 323.15 to 423.15 K and Pressure of up to 20 MPa.* Journal of Chemical & Engineering Data, 2016. **61**(10): p. 3573-3584.
[43]. Hou, S.-X., G.C. Maitland, and J.M. Trusler, *Phase equilibria of (CO 2+ H 2 O+ NaCl) and (CO 2+ H 2 O+ KCl): measurements and modeling.* The Journal of Supercritical Fluids, 2013. **78**: p. 78-88.
[44]. Takenouchi, S. and G.C. Kennedy, *The solubility of carbon dioxide in NaCl solutions at high temperatures and pressures.* American journal of science, 1965. **263**(5): p. 445-454.
[45]. Bando, S., F. Takemura, M. Nishio, E. Hihara, and M. Akai, *Solubility of CO2 in aqueous solutions of NaCl at (30 to 60) C and (10 to 20) MPa.* Journal of Chemical & Engineering Data, 2003. **48**(3): p. 576-579.
[46]. Yan, W., S. Huang, and E.H. Stenby, *Measurement and modeling of CO 2 solubility in NaCl brine and CO 2–saturated NaCl brine density.* International Journal of Greenhouse Gas Control, 2011. **5**(6): p. 1460-1477.
[47]. Tang, Y., X. Bian, Z. Du, and C. Wang, *Measurement and prediction model of carbon dioxide solubility in aqueous solutions containing bicarbonate anion.* Fluid Phase Equilibria, 2015. **386**: p. 56-64.
[48]. Markham, A.E. and K.A. Kobe, *The solubility of carbon dioxide and nitrous oxide in aqueous salt solutions.* Journal of the American Chemical Society, 1941. **63**(2): p. 449-454.
[49]. Liu, Y., M. Hou, G. Yang, and B. Han, *Solubility of CO 2 in aqueous solutions of NaCl, KCl, CaCl 2 and their mixed salts at different temperatures and pressures.* The Journal of supercritical fluids, 2011. **56**(2): p. 125-129.

[50]. Tong, D., J.M. Trusler, and D. Vega-Maza, *Solubility of CO2 in aqueous solutions of CaCl2 or MgCl2 and in a synthetic formation brine at temperatures up to 423 K and pressures up to 40 MPa.* Journal of Chemical & Engineering Data, 2013. **58**(7): p. 2116-2124.
[51]. Stewart, P.B. and P.K. Munjal, *Solubility of carbon dioxide in pure water, synthetic sea water, and synthetic sea water concentrates at-5. deg. to 25. deg. and 10-to 45-atm. pressure.* Journal of Chemical and Engineering data, 1970. **15**(1): p. 67-71.
[52]. Yasunishi, A. and F. Yoshida, *Solubility of carbon dioxide in aqueous electrolyte solutions.* Journal of Chemical and Engineering Data, 1979. **24**(1): p. 11-14.
[53]. Li, Z., M. Dong, S. Li, and L. Dai, *Densities and solubilities for binary systems of carbon dioxide+ water and carbon dioxide+ brine at 59 C and pressures to 29 MPa.* Journal of Chemical & Engineering Data, 2004. **49**(4): p. 1026-1031.
[54]. Wagner, W. and H.-J. Kretzschmar, *IAPWS industrial formulation 1997 for the thermodynamic properties of water and steam.* International Steam Tables: Properties of Water and Steam Based on the Industrial Formulation IAPWS-IF97, 2008: p. 7-150.
[55]. Lewis, E. and R. Perkin, *The Practical Salinity Scale 1978: conversion of existing data.* Deep Sea Research Part A. Oceanographic Research Papers, 1981. **28**(4): p. 307-328.
[56]. Span, R. and W. Wagner, *A new equation of state for carbon dioxide covering the fluid region from the triple-point temperature to 1100 K at pressures up to 800 MPa.* Journal of physical and chemical reference data, 1996. **25**(6): p. 1509-1596.
[57]. Chladni, E.F.F., *Entdeckungen über die Theorie des Klanges*. 1787: Zentralantiquariat der DDR.
[58]. Haghighi, H., A. Chapoy, R. Burgess, S. Mazloum, and B. Tohidi, *Phase equilibria for petroleum reservoir fluids containing water and aqueous methanol solutions: Experimental measurements and modelling using the CPA equation of state.* Fluid Phase Equilibria, 2009. **278**(1): p. 109-116.
[59]. Haghighi, H., A. Chapoy, R. Burgess, and B. Tohidi, *Experimental and thermodynamic modelling of systems containing water and ethylene glycol: Application to flow assurance and gas processing.* Fluid Phase Equilibria, 2009. **276**(1): p. 24-30.
[60]. Chapoy, A., S. Mazloum, R. Burgass, H. Haghighi, and B. Tohidi, *Clathrate hydrate equilibria in mixed monoethylene glycol and electrolyte aqueous solutions.* The Journal of Chemical Thermodynamics, 2012. **48**: p. 7-12.
[61]. Vilcu, R. and I. Gainar, *Loslichkeit der gase unter druck in flussigkeiten. i. das system kohlendioxid-wasser.* Revue Roumaine de Chimie, 1967. **12**(2): p. 181-&.
[62]. Bamberger, A., G. Sieder, and G. Maurer, *High-pressure (vapor+ liquid) equilibrium in binary mixtures of (carbon dioxide+ water or acetic acid) at temperatures from 313 to 353 K.* The Journal of Supercritical Fluids, 2000. **17**(2): p. 97-110.
[63]. Savelyeya, S.D.M.a.N.I., *The solubility of CO2 in NaCl and CaCl2 solutions at 25, 50, and 75 °C under elevated CO2 pressures.* Geokhimiya, 1972. **6**.
[64]. Setschenow, J., *Über die konstitution der salzlösungen auf grund ihres verhaltens zu kohlensäure.* Zeitschrift für Physikalische Chemie, 1889. **4**(1): p. 117-125.
[65]. Görgényi, M., J. Dewulf, H. Van Langenhove, and K. Héberger, *Aqueous salting-out effect of inorganic cations and anions on non-electrolytes.* Chemosphere, 2006. **65**(5): p. 802-810.
[66]. Millero, F.J., F. Huang, and A.L. Laferiere, *Solubility of oxygen in the major sea salts as a function of concentration and temperature.* Marine chemistry, 2002. **78**(4): p. 217-230.

Supporting Information

CO_2 Solubility in formation water under sequestration conditions

Pezhman Ahmadi[a], Antonin Chapoy[a,b,]*

[a] *Hydrates, Flow Assurance & Phase Equilibria Research Group, Institute of Petroleum Engineering, Heriot-Watt University, Edinburgh EH14 4AS, Scotland, UK*

[b] *Mines ParisTech, CTP – Centre Thermodynamique des procédés, 35 rue St Honoré 77305 Fontainebleau, France*

[*] Corresponding author, Email: a.chapoy@hw.ac.uk

Results for solubility of CO_2 in mixed salts aqueous solution:

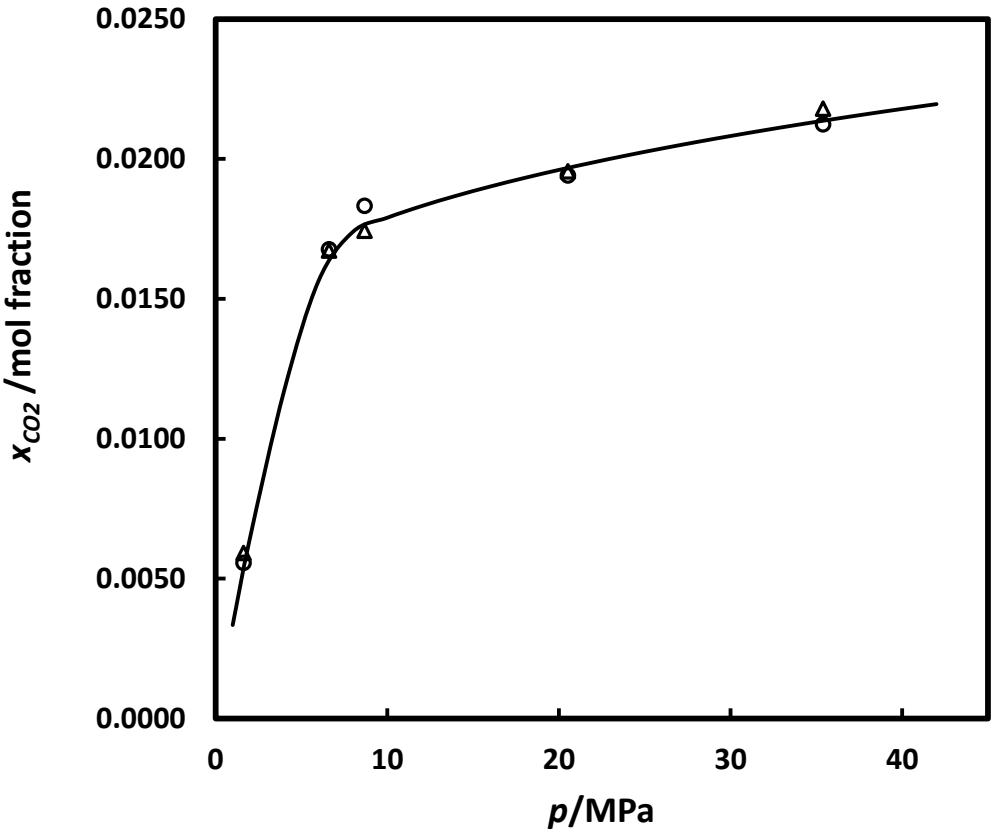

Figure 10. Mole fraction of CO_2 dissolved in the mixed salts aqueous solution at 303.16 K. This work (O), Models: Duan (∆), sCPA-EoS (—).

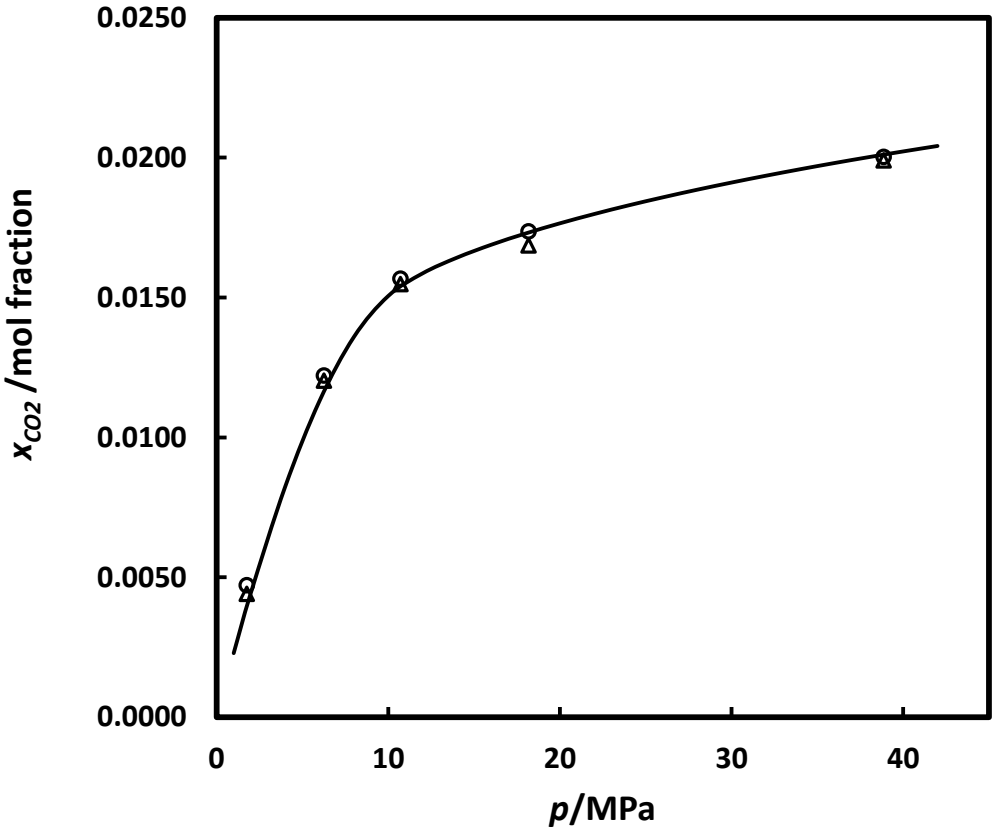

Figure 11. Mole fraction of CO_2 dissolved in the mixed salts aqueous solution at 323.20 K. This work (O), Models: Duan (∆), sCPA-EoS (—).

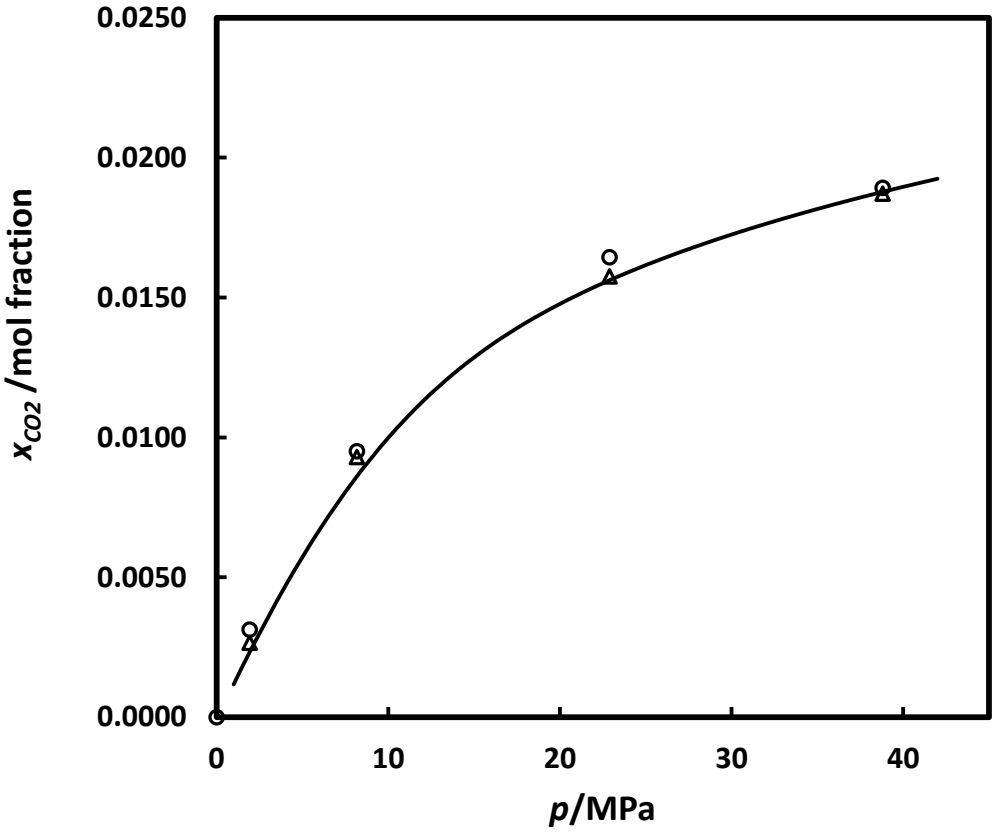

Figure 12. Mole fraction of CO_2 dissolved in the mixed salts aqueous solution at 373.19 K. This work (O), Models: Duan (∆), sCPA-EoS (—).

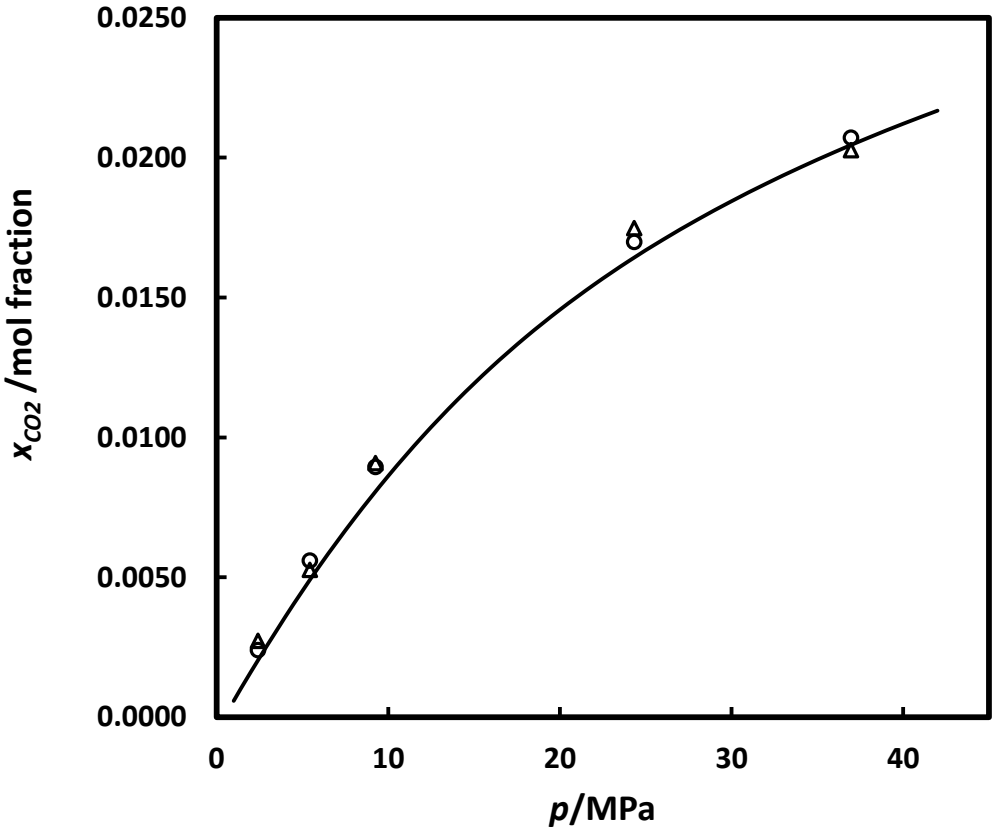

Figure 13. Mole fraction of CO_2 dissolved in the mixed salts aqueous solution at 423.19 K. This work (O), Models: Duan (∆), sCPA-EoS (—)